RSC Advances

PAPER

View Article Online
View Journal | View Issue

Cite this: *RSC Adv.*, 2025, **15**, 3448

Impact of pharmacokinetic enhancement strategies on the antimicrobial and antioxidant activities of hydroxytyrosol†

Giuliana Prevete,[a] Elisa Scipioni,[a] Enrica Donati,[a] Noemi Villanova,[b] Andrea Fochetti,[b] Laura Lilla,[a] Stefano Borocci,[cd] Roberta Bernini*[b] and Marco Mazzonna*[a]

Hydroxytyrosol (HTyr), a plant-derived phenolic compound found in *Olea europaea* L. products and by-products, is well-known for its antioxidant activity and a wide range of biological effects, including anti-inflammatory, anticancer, antiviral, cardioprotective, neuroprotective, and antibacterial properties. However, due to its high hydrophilicity, HTyr exhibits unfavorable pharmacokinetic properties, preventing its potential therapeutic use. Various strategies can be employed to address these limitations. In this study, we evaluated the effect of two specific approaches on the HTyr antimicrobial and antioxidant activities: chemical modification of HTyr by lipophilization of the alcoholic moiety and encapsulation in liposomes. Based on our experience in the synthesis and biological activities of HTyr derivatives, the attention was focused on HTyr oleate (HTyr-OL), having a C-18 unsaturated alkylic chain responsible for an increased lipophilicity compared to HTyr. This structural feature enhanced antimicrobial activity against both tested strains of *S. aureus*, ATCC 25923 (wild-type strain) and ATCC 33591 (MRSA), and comparable antioxidant activity against two different radicals, Galvinoxyl radical and 1,1-diphenyl-2-picrylhydrazyl radical. Moreover, liposomes as delivery systems for HTyr and HTyr-OL were developed using both natural and synthetic amphiphiles, and the impact of encapsulation on their activities was further investigated. The experimental results showed that the antimicrobial properties of HTyr and HTyr-OL against *S. aureus* strains were not enhanced after encapsulation in liposomes, while the high antioxidant activity of HTyr-OL was preserved when conveyed in liposomes.

Received 19th November 2024
Accepted 27th January 2025

DOI: 10.1039/d4ra08205b

rsc.li/rsc-advances

1. Introduction

Hydroxytyrosol (HTyr) is a plant-derived phenolic compound, primarily found in *Olea europaea* L. products and by-products (Chart 1). It is notably present in extra virgin olive oil,[1,2] as well as in olive by-products such as leaves[3,4] and olive mill wastewater.[5,6] In these matrices, HTyr is mainly found in the form of secoiridoid derivatives, including oleuropein, its aglycone form, verbascoside, and oleacin. HTyr free form results from the hydrolytic activity of endogenous β-glucosidase[7] during olives ripening, olive oil production, and storage over time.[8]

Several *in vivo* and *in vitro* studies have confirmed that HTyr displays a wide range of biological activities,[2,9,10] including antioxidant,[10] cardioprotective,[11] neuroprotective,[10,12–14] anticancer,[15–19] anti-inflammatory,[10,18–20] antidiabetic,[21] and antimicrobial properties.[3] Given these attractive features, an increasing number of research groups have focused on synthesizing HTyr and obtaining HTyr-rich extracts from olive oil by-products.[22] Specifically, HTyr can be recovered from waste products using environmentally and economically sustainable technologies, which align with the principles of green chemistry and the circular economy, enabling its reuse and valorization in various application fields.[23–25]

Despite the positive effects of HTyr on human health, its potential therapeutic use is limited by several physicochemical factors that affect its absorption, distribution, metabolism, excretion processes, stability, and biological activity.[26–28] In particular, the problematic absorption[29] of HTyr is primarily related to its very high solubility in aqueous media and

[a]*CNR-Institute for Biological Systems (ISB), Research Area of Rome 1, Strada Provinciale 35d, n. 9, 00010 Montelibretti, Roma, Italy. E-mail: giuliana.prevete@isb.cnr.it; eliscipi@gmail.com; enrica.donati@cnr.it; laura.lilla@cnr.it; marco.mazzonna@cnr.it*

[b]*Department of Agriculture and Forest Sciences (DAFNE), University of Tuscia, 01100 Viterbo, Italy. E-mail: noemi.villanova@unitus.it; andrea.fochetti@unitus.it; roberta.bernini@unitus.it*

[c]*Department for Innovation in Biological, Agrofood and Forest Systems (DIBAF), University of Tuscia, 01100 Viterbo, Italy*

[d]*CNR-Institute for Biological Systems (ISB) – Secondary Office of Rome-Reaction Mechanisms c/o Department of Chemistry, La Sapienza University of Rome, Rome, Italy. E-mail: borocci@unitus.it*

† Electronic supplementary information (ESI) available. See DOI: https://doi.org/10.1039/d4ra08205b

biological fluids,[30] poor stability in the gastrointestinal tract,[31] low permeation through the small intestine epithelial cells, and extensive and rapid metabolic reactions.[32] To address these limitations, researchers are exploring innovative strategies to enhance HTyr bioavailability and plasma half-life.[33] Among these, esterification of the alcoholic hydroxyl group of HTyr has emerged as a promising approach. In fact, this method introduces a saturated, mono-, or polyunsaturated alkyl chain, leading to the formation of the so-called "phenolipids" or "lipophenols". By synthesizing HTyr esters with C2–C18 acyl chains, researchers aim to improve HTyr's lipophilicity while preserving its biological properties, thereby creating new opportunities for applications in pharmaceutical, nutraceuticals, and food fields.[34–37]

Among the HTyr derivatives studied so far, HTyr oleate (HTyr-OL, Chart 1) stands out as one of the most interesting and promising. HTyr-OL is a fatty ester having a C18:1 alkyl chain, responsible for a significantly increased lipophilicity ($\log K_{OW} > 3.3$) compared to HTyr ($\log K_{OW} = 0.809$),[38] while maintaining the catechol moiety accountable for its biological activities.[39,40]

HTyr-OL can also be considered a surfactant due to its amphiphilic structure, which features a hydrophilic head derived from the HTyr catechol moiety and a hydrophobic tail provided by the C18:1 chain. In aqueous solutions, dispersed HTyr-OL molecules may aggregate to form micelles when the concentration of surfactant molecules exceeds the critical micelle concentration (cmc), defined as the concentration of surfactants in free form in equilibrium with those in aggregated form in solution. Micelles take form by orienting the hydrophobic portions of surfactants molecules toward the micelle core, while the hydrophilic head groups face the surrounding aqueous phase.

Alternatively, the limitations of HTyr can be addressed through nanotechnologies. Incorporating natural compounds like HTyr into various delivery systems has been shown to be an effective strategy to enhance stability, solubility, and bioavailability, also preventing degradation caused by environmental conditions (pH, enzymatic activity, or oxygen exposure). This approach also enhances the targeting of loaded compounds, thereby minimizing interactions with other components in the human body and reducing the risk of systemic side effects. In particular, liposomes represent promising and versatile delivery systems for bioactive compounds due to their biodegradability, low toxicity, and versatility in entrapping lipophilic, hydrophilic, and amphiphilic compounds.[41,42] They can also be functionalized for targeted delivery.[43]

In this study, we report on an investigation aimed at analyzing how these two strategies, chemical modification of HTyr and encapsulation of HTyr or HTyr-derivative in liposomes, designed to overcome the pharmacokinetic limitations of HTyr, affect antimicrobial and antioxidant properties.

For the chemical modification approach, HTyr-OL was tested as an acyl derivative of HTyr with enhanced lipophilicity. Its amphiphilic nature was characterized by determining its cmc and simulating micelle formation through Molecular Dynamic Simulations. Both HTyr and HTyr-OL were synthesized in our laboratories.

For the liposomal conveyance approach, delivery systems containing HTyr or HTyr-OL were formulated using natural phospholipids with varying alkyl chain lengths: 1,2-dioleoyl-*sn*-glycero-3-phosphocholine (C18:1, DOPC), 1,2-dipalmitoyl-*sn*-glycero-3-phosphocholine (C16:0, DPPC), or 1,2-dimyristoyl-*sn*-glycero-3-phosphocholine (C14:0, DMPC). These formulations were prepared either with or without cholesterol (Chol) or a synthetic cationic lipid (LIPCAT) (Chart 1).

Liposomes were characterized considering size, polydispersity index, ζ-potential, and entrapment efficiency. Additionally, their stability over time and at different pH values was evaluated, along with the controlled release of entrapped HTyr.

Finally, the antimicrobial and antioxidant properties of HTyr and HTyr-OL, in both free form and embedded in liposomes, were investigated *in vitro*. Specifically, the antimicrobial activity was evaluated against two strains of *Staphylococcus aureus*: ATCC 25923 (wild type strain) and ATCC 33591 (methicillin-resistant strain, MRSA). Antioxidant capacity was analyzed by determining the kinetic rate constants of hydrogen atom transfer reactions to two different radicals: 2,6-di-*tert*-butyl-α-(3,5-di-*tert*-butyl-4-oxo-2,5-cyclohexadien-1-ylidene)-*p*-tolyloxy

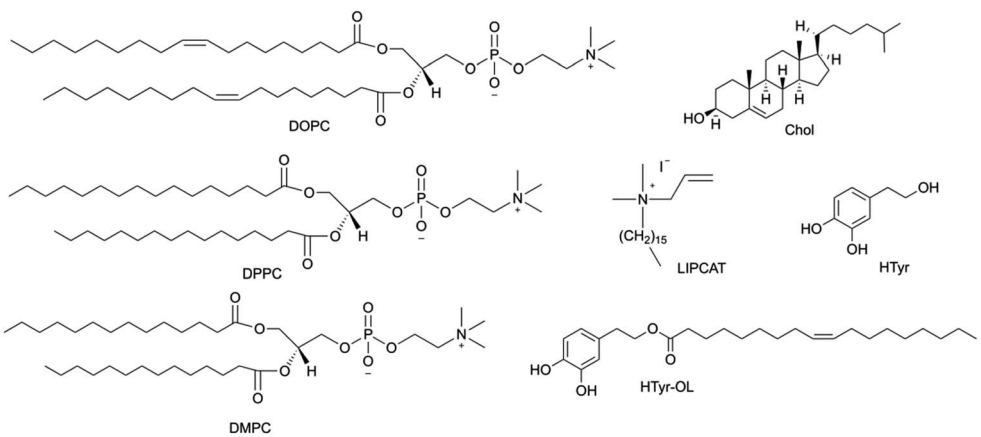

Chart 1 Chemical structures of HTyr, HTyr-OL and lipid components of developed liposomes.

(galvinoxyl free radical, GO$^{\bullet}$) and 1,1-diphenyl-2-picrylhydrazyl radical (DPPH$^{\bullet}$).

Furthermore, the potential of HTyr-OL to exert antioxidant activity when integrated as a component of the lipid bilayer in liposomes was investigated.

2. Materials and methods

2.1 Chemicals and solvents

Natural phospholipids 1,2-dioleoyl-*sn*-glycero-3-phosphocholine (C18:1, DOPC), 1,2-dipalmitoyl-*sn*-glycero-3-phosphocholine (C16:0, DPPC) and 1,2-dimyristoyl-*sn*-glycero-3-phosphocholine (C14:0, DMPC) were purchased from Avanti Polar Lipids (Alabaster, AL, USA).

Cholesterol (Chol, purity 99%), 4-methylbenzophenone, 2,2′-azino-bis(3-ethylbenzothiazoline-6-sulfonic acid) diammonium salt (ABTS, purity ≥98%), 2,6-di-*tert*-butyl-α-(3,5-di-*tert*-butyl-4-oxo-2,5-cyclohexadien-1-ylidene)-*p*-tolyloxy (galvinoxyl free radical, GO$^{\bullet}$), 1,1-diphenyl-2-picrylhydrazyl radical (DPPH$^{\bullet}$), potassium persulfate (purity >99%), sodium hydroxide (NaOH, purity 98%), phosphate-buffered saline tablet (PBS; 0.01 M phosphate buffer, 0.0027 M KCl, 0.137 M NaCl, pH 7.4, at 25 °C, prepared by dissolving 1 tablet in 200 mL of deionized water), cellulose dialysis membrane (D9527-100FT, molecular weight cut off = 14 kDa) were purchased from Sigma-Aldrich (St. Louis, MO, USA).

HTyr was synthesized according to a patented procedure already optimized by us.[44] HTyr-OL was obtained by esterification of HTyr with oleyl chloride as recently described by us.[45]

The cationic amphiphile allyl-hexadecyl-dimethyl-ammonium iodide (LIPCAT) was synthetized following a procedure reported in the literature.[46]

Solvents (HPLC grade) were purchased from VWR International S.r.l. (Milan, Italy) and Romil Pure Chemistry (Cambridge, UK). Hydrochloric acid (HCl 37%) and formic acid were supplied by Carlo Erba (Milan, Italy). Deuterated chloroform ($CDCl_3$) was provided by Eurisotop (Cambridge Isotope Laboratories, Tewksbury, MA, USA). Muller–Hinton (MH) broth and MH agar were purchased from Fisher Scientific (Milan, Italy).

2.2 Determination of the cmc for HTyr-OL

The cmc of HTyr-OL was determined using a Zetasizer Nano ZS equipped with a 4 mW He–Ne laser operating at a wavelength of 632.8 nm. The scattered light was detected at an angle of 173°, an optical arrangement that maximizes the detection of scattered light while maintaining signal quality. This setup provides the exceptional sensitivity required to measure the size of entities such as nanoparticles at low concentrations.[47]

The HTyr-OL stock solution (1 mM) was prepared in H_2O by sonication in a bath sonicator (Elmasonic S 30H) for 90 min, followed by stirring on a magnetic plate carried out at room temperature for 30 min. Afterwards, the HTyr-OL stock solution was filtered using MS® Nylon Syringe Filters (13 mm × 0.45 μm) to break any aggregates that had formed.

The HTyr-OL stock solution was then diluted in H_2O to obtain solutions with concentration ranging from 2×10^{-3} to 5 μM. Closed polystyrene cuvettes were filled with 1 mL of each HTyr-OL diluted concentration prepared.

Before performing DLS measurements, an optimization stage was carried out for each solution to determine the best experimental conditions, such as cells position, number of runs, run duration and attenuator settings. The optimized parameters (cell position = 4.65 nm, number of runs = 12, runs duration = 10 s, attenuator = 11) were then manually introduced to override the default software settings. All measurements were performed at 25 °C in triplicate. Data were collected as the intensity of scattered light (k_{cps}) *versus* HTyr-OL concentration (μM).

2.3 Molecular dynamics simulation

The initial configuration of the simulated system was built by placing 50 molecules of HTyr-OL with a random orientation and 2823 water molecules in a cubic box of $4.92 \times 4.92 \times 4.92$ nm^3.

The molecular dynamics simulations were performed using GROMACS package (version 2020.5)[48] with the CHARMM36 (ref. 49) to describe the bonding and non-bonding interactions of the surfactant molecules. Water was modelled with the TIP3P model.[50] Non-bonding interactions were calculated using a cut-off of 1.2 nm. The particle mesh Ewald (PME) method was applied to the long-range electrostatic interactions. The systems were energy minimized and equilibrated at 298 K and 1 bar by using the velocity-rescale thermostat[51] and Parrinello–Rahman barostat.[52] The system was simulated for 100 ns.

2.4 Liposomes preparation

Liposomes were prepared according to the lipid film hydration protocol, followed by a freeze–thaw procedure and extrusion process.[53,54] Liposomes were formulated with a natural phosphocholine (DOPC, DMPC, or DPPC) in the presence or absence of cholesterol (Chol) or a cationic synthetic amphiphile LIPCAT (Chart 1).

An appropriate amount of lipid components (DOPC/DMPC/DPPC, Chol, LIPCAT, HTyr-OL) was dissolved in $CHCl_3$ in a round bottom flask. To prepare HTyr loaded liposomes, HTyr was dissolved in MeOH and added to the lipid mixture to achieve a molar ratio of 1 : 8 HTyr/lipids. Subsequently, the solution was dried by rotary evaporation (BUCHI R-200) and then under high vacuum for 5 h to remove any traces of organic solvents, resulting in a thin lipid film.

In all cases, the film was hydrated with a phosphate buffer saline solution (PBS, 150 mM), producing a liposomal suspension with a total lipid concentration of either 10 mM or 20 mM, depending on the specific formulation.

To completely detach the lipid film from the flask, the aqueous suspension was vortexed, and the resulting multilamellar vesicles were freeze–thawed five times, from liquid nitrogen to 50 °C.[55]

Liposomal dispersions were then extruded (GJE-10 mL) ten times under high pressure through a 100 nm pore size polycarbonate membrane (Whatman Nucleopore) at a temperature above their transition temperatures (T_m) to obtain small unilamellar vesicles. Specifically, due to the formulation method,

the transition temperatures of our liposomes are expected to be similar to those of the main lipid used in large excess: DOPC ($T_m \sim -16.5$ °C), DMPC ($T_m \sim 23.6$ °C), and DPPC ($T_m \sim 41.4$ °C).

Lastly, to remove any component not incorporated into the liposomes, all liposomal suspensions were subjected to dialysis against PBS (150 mM) using a buffer volume 25 times greater than the total sample volume, with the system kept under gentle magnetic stirring.

2.5 Liposomes physicochemical characterization

2.5.1 Size and ζ-potential measurements. The hydrodynamic diameter, polydispersity index (PDI) and ζ-potential of all developed liposomes were determined through Dynamic and Electrophoretic Light Scattering (DLS, ELS) measurements using a Zetasizer Nano ZS equipped with a 5 mV He/Ne laser ($\lambda = 632.8$ nm) and a thermostated cell holder. The temperature was set at 25 °C for all measurements.

Particle size distribution and PDI were measured based on backscatter detection of scattered light at an angle of 173°. The measured autocorrelation function was analyzed by using the cumulant fit. The first cumulant was used to obtain the apparent diffusion coefficients (D) of the particles, which were then converted into apparent hydrodynamic diameters (D_h) using the Stokes–Einstein relationship:

$$D_h = \frac{k_B T}{3\pi\eta D} \quad (1)$$

where $k_B T$ is the thermal energy and η is the solvent viscosity.

The ζ-potential of liposomes was determined by ELS measurements, and low voltages were applied to avoid the risk of Joule heating effects. To determine the electrophoretic mobility, doppler shift analysis was performed using phase analysis light scattering (PALS)[56] a method useful at high ionic strengths where mobilities are usually low. The mobility (μ) of the liposomes was converted into ζ-potential using the Smoluchowski relation $\zeta = \mu\eta/\varepsilon$, where ε is the permittivity and η is the viscosity of the solution.

All liposomal suspensions were diluted to a total lipid concentration of 1 mM in PBS (150 mM) for DLS measurements, and in diluted PBS (15 mM) for ELS measurements.

2.5.2 Determination of HTyr entrapment efficiency in liposomes. The amount of HTyr embedded in liposomes was determined by UPLC-PDA analysis, following the procedure described below.

Before UPLC measurements, liposomes were properly diluted with MeOH to obtain their disruption and the complete lipids solubilization. All samples were then filtered through polytetrafluoroethylene (PTFE) membranes (4 mm × 0.2 μm) injection.

An Acquity UPLC HSS T3 column (1.8 μm, 150 × 2.1 mm id) was employed using as mobile phases water (0.1% (v/v) formic acid, phase A) and acetonitrile (0.1% (v/v) formic acid, phase B), which were eluted according to the following gradient: 0–3 min from 85% phase A and 15% phase B to 82% phase A and 18% phase B; 3–6.5 min from 82% phase A and 18% phase B to 77% phase A and 23 & phase B; 6.5–10 min from 77% phase A and 23% phase B to 40% phase A and 60% phase B; 10–11 min from 40% phase A and 60% phase B to 100% phase B until the minutes 22. The optimum flow rate was 0.4 mL min^{-1} while the injection volume was 2 μL. The detection wavelength was set at 280 nm for HTyr.

According to the calibration curve, $y = 5 \times 10^6 x - 11.180$ (Fig. S1†), the entrapment efficiency (EE%) of HTyr entrapped in liposomes was calculated using the following equation:

$$EE(\%) = \frac{[HTyr]_{pd}}{[HTyr]_0} \times 100 \quad (2)$$

where $[HTyr]_{pd}$ indicates the concentration of HTyr after liposome purification by dialysis and $[HTyr]_0$ corresponds to its concentration soon after liposome extrusion.

2.5.3 Determination of HTyr-OL concentration in liposomes. HTyr-OL in liposomes was quantified by ^{1}H-NMR analysis, using a Bruker AVANCE 600 NMR spectrometer operating at the proton frequency of 600.13 MHz. All NMR spectra were recorded at 27 °C.

Briefly, 1 mL of each liposome suspension was freeze dried, and the residue was solubilized in 0.9 mL of $CDCl_3$. Then, 0.1 mL of a 4-methylbenzophenone solution (10 mM in $CDCl_3$) was added as internal standard (IS) in the sample, achieving a final IS concentration equal to 1 mM. 4-Methylbenzophenone was chosen as the IS because it provides well-separated signals without interfering with the signals of the liposome constituents in the NMR spectra. The solution was then filtered through polytetrafluoroethylene (PTFE) membranes (4 mm × 0.2 μm) to remove the inorganic salts present in the PBS buffer solution.

For quantitative purposes, the multiplet signal at 7.730–7.716 ppm of 4-methylbenzophenone was selected as the reference signal because it did not overlap with other signals in the spectra. The signals used for HTyr-OL quantification in liposomes were identified by comparison with the reference sample of the molecule dissolved in $CDCl_3$.

2.5.4 *In vitro* release of HTyr from liposomes. The forced release of HTyr from liposomes was evaluated by dialysis method (PBS volume 50 times the total volume of the sample) under magnetic stirring.[57]

Samples were collected every hour over a period of 24 hours; the collected liposomal aliquots were diluted with MeOH (1 : 1 v/v) and filtrated through PTFE membranes (4 mm × 0.2 μm).

Finally, the percentage of HTyr leakage from liposomes at a specific time up to 24 h was determined by chromatographic analyses as described above.

2.5.5 Assessment of stability. The physical stability of all developed liposomes was evaluated over 28 days of storage at 4 °C, protected from light sources, by determining vesicles dimensions and PDI values by DLS measurements.

Furthermore, liposomes stability was investigated at different pH values by adding appropriate volumes of HCl or NaOH aqueous solutions to the liposome suspensions in PBS. To this purpose, the pH was adjusted to mimic the values found in the human digestive system,[58] considering the physiological transit times. In particular, liposome dimensions and PDI were evaluated after incubation at pH 5.7 for 1–3 min (mouth), at pH

2.9 for 30 min–3 h (stomach), at pH 6.4 for 3 h (intestine), and at pH 8 for 24 h (colon). All collected results were compared with those obtained at pH 7.4 in PBS (150 mM).

2.6 Minimum inhibitory concentration and minimum bactericidal concentration determination

The *in vitro* antimicrobial activity of HTyr embedded in liposomes and HTyr-OL, either in its free form or added as a component of the lipid bilayer in liposomes, was assessed through the microdilution method[59] determining the Minimum Inhibitory Concentration (MIC) and the Minimum Bactericidal Concentration (MBC) against two strains of *Staphylococcus aureus*: ATCC 25923 (wild type strain) and ATCC 33591 (methicillin-resistant *S. aureus*, MRSA).

Gentamicin was tested as a control against both bacteria strains at a concentration of 5 μg mL^{-1}, demonstrating a bactericidal effect against ATCC 25923 strain and an inhibitory effect on ATCC 33591 strain, as already reported in the literature.

The antimicrobial activity of HTyr in free form was previously investigated in a prior study reported in the literature.[3] Additionally, the activity of empty liposomes was also examined against both bacteria strains under investigation.

An overnight culture of ATCC 25923 and ATCC 33591 was prepared in Muller–Hinton (MH) broth and incubated at 37 °C. The following day, the inoculum was diluted in MH broth, measuring the optical density (OD) of 10-fold serial dilutions at 600 nm (UV-2401PC) to reach a final organism density of 2–8 × 10^5 CFU mL^{-1}. Both diluted cultures were aliquoted in a flat bottom 96 well per plate, and the antimicrobial agent was added, in triplicates, at different concentrations. The plates were incubated overnight at 37 °C. Afterwards, plates were examined and all the transparent wells, potentially corresponding to the MIC values, were plated on fresh MH agar plates kept at 37 °C overnight. Growth inhibition in each 96 well per plate was compared to the growth positive control of each bacteria strain. After 24 hours, the MH agar plates were observed, and those showing bacterial growth were annotated as MIC, while plates showing no bacterial growth were annotated as MBC.

2.7 Spectrophotometric kinetic studies

The kinetic rate constant of the Hydrogen Atom Transfer (HAT) reactions from HTyr or HTyr-OL, in their free form, to 2,6-di-*tert*-butyl-α-(3,5-di-*tert*-butyl-4-oxo-2,5-cyclohexadien-1-ylidene)-*p*-tolyloxy (galvinoxyl free radical, GO$^\bullet$) and 1,1-diphenyl-2-picrylhydrazyl radical (DPPH$^\bullet$) were investigated in CH_3CN at 25 °C according to the procedure reported in the literature.[60]

For the reaction with GO$^\bullet$ (20 μM), different aliquots of HTyr (final concentration 0.21–1.47 mM) or HTyr-OL (final concentration 0.21–1.22 mM) solutions were added to the solution of the radical in spectrophotometric quartz cuvettes (12.5 mm × 45 mm × 12.5 mm, d = 10 mm, V = 3.5 mL).

For the reaction with DPPH$^\bullet$ (80 μM), aliquots of HTyr (final concentration 0.40–3.24 mM) or HTy-OL (final concentration 0.81–3.24 mm) solutions were added to the DPPH$^\bullet$ (80 μM) solution in quartz cuvettes (12.5 mm × 45 mm × 12.5 mm, d = 10 mm, V = 3.5 mL).

The measurements were carried out by recording the absorbance variations at 428 and 517 nm (UV-2401PC) for the reaction with GO$^\bullet$ and DPPH$^\bullet$, respectively.

For both substrates investigated, each kinetic trace followed a pseudo-first-order decay and k_{obs} values were obtained by exponential fitting of the absorbance decay traces. The second-order rate constants, k_H, were obtained from the slopes of the linear plots of k_{obs} *vs.* substrate concentration. The k_H values determined are expressed as the average of at least two independent experiments.

In the absence of the substrate, the decay of the absorbance for both radicals was negligible over the kinetic time scale.

2.8 Evaluation of HTyr-OL based liposomes antioxidant activity by ABTS$^{\bullet+}$

The amount of catechol residues exposed on the external surface of HTyr-OL functionalized liposomes was determined by exploiting the reaction with the ABTS radical cation (ABTS$^{\bullet+}$).[61]

ABTS$^{\bullet+}$ was produced by reacting a 7 mM ABTS solution with 2.45 mM potassium persulfate in water, keeping the mixture under stirring overnight at room temperature in the dark. Afterwards, the ABTS$^{\bullet+}$ solution was diluted in PBS (15 mM) to obtain an absorbance value of 0.70 ± 0.02 at 734 nm (UV-2401PC).

HTyr-OL was used as a reference standard to create a calibration curve. In particular, different concentration of HTyr-OL (0.00193–0.1115 mM) were reacted with the diluted ABTS$^{\bullet+}$ solution in a spectrophotometric cuvette.

The absorbance of the reaction solution was measured at 734 nm (UV-2401PC) before adding HTyr-OL and exactly 10 min after the initial mixing. The percentage of ABTS$^{\bullet+}$ inhibition (-$\%_{inhibition}$) triggered by HTyr-OL was determined according to the following equation:

$$\%_{inhibition} = \frac{A_0 - A_t}{A_0} \times 100 \quad (3)$$

where A_0 is the initial absorbance recorded for ABTS$^{\bullet+}$ solution alone and A_t is the absorbance recorded after 10 min of reaction of HTyr-OL with ABTS$^{\bullet+}$. HTyr-OL calibration curve, $y = 1269x + 2.265$ (Fig. S2†), was made plotting the $\%_{inhibition}$ as a function of the different μmol of HTyr-OL added in cuvette.

Furthermore, 20 μL of HTyr-OL based liposomes were added to 1 mL of diluted ABTS$^{\bullet+}$ solution in the cuvette, and the reduction in absorbance was measured at 734 nm (UV-2401PC) before and after 10 min of reaction. The $\%_{inhibition}$ determined for HTyr-OL based liposomes was expressed as μmol of HTyr-OL equivalents present inside the volume of liposome formulation tested, which was finally converted to the concentration (mM) of catechol residues actually exposed on the surface of the HTyr-OL based liposomes developed.

2.9 Membrane fluidity studies by DLS

The membrane fluidity of DPPC/Chol/HTyr-OL and DMPC/Chol/HTyr-OL liposomes was investigated by performing DLS measurements using a Nano Zetasizer ZS.[62–64]

Firstly, an optimization stage was carried out to assess the best experimental conditions, such as cells positions, number of runs, duration of runs and attenuator settings. The optimized parameters (cell position = 1.05 nm, number of runs = 14, duration of runs = 10 s, attenuator position = 3) were then introduced and locked manually to override the default software settings. Furthermore, the detection of the scattered light was set at an angle of 173° for backscatter detection.

A closed quartz cuvette (12.5 mm × 45 mm × 12.5 mm, $d = 10$ mm, $V = 3.5$ mL) was filled with 1 mL of each liposomal suspension (10 mM in total lipid concentration), and the mean count rate was collected between 20 °C and 60 °C for DPPC/Chol/HTyr-OL liposomes and between 12 °C and 40 °C for DMPC/Chol/HTyr-OL liposomes, respectively, in steps of 1 °C. For each temperature step, two independent measurements were performed, preceded by an equilibration temperature time of 180 s.

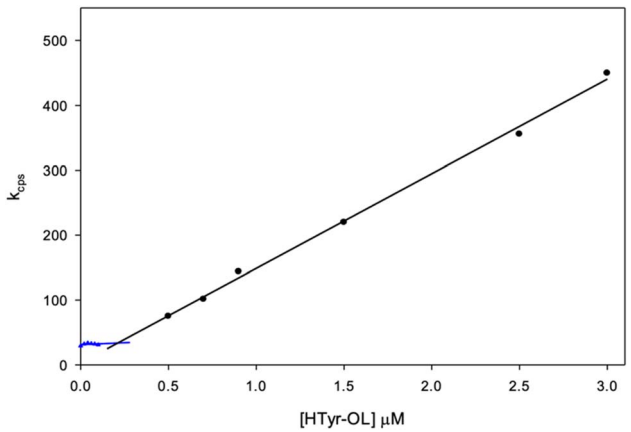

Fig. 1 Plot of the intensity of scattered light (k_{cps}) as a function of HTyr-OL concentration (μM).

3. Results and discussion

3.1 HTyr-OL cmc determination

Due to the amphiphilic nature of HTyr-OL, its behavior in water was analyzed through DLS measurements to determine its cmc. DLS is a technique well suited to evaluate the cmc of surfactants, representing a valid alternative to methods based on conductivity, surface tension, and fluorescence measurements.[65–67]

The determination of HTyr-OL cmc was performed in water observing the variation in the intensity of scattered light (expressed in kilocounts per second, k_{cps}) as a function of HTyr-OL concentration, which ranged from 2×10^{-3} μM to 5 μM. As shown in the Fig. 1, the intensity of scattered light detected for HTyr-OL concentrations below the cmc (blue linear plot) remains approximately constant and corresponds to that of deionized water. Once the cmc is reached, HTyr-OL starts to aggregate in the aqueous solution, forming micelles, and the light begins to scatter. At this point the intensity of scattered light increases linearly with rising HTyr-OL concentration (black linear plot). Finally, HTyr-OL cmc is determined by the intersection of the two linear fits and corresponds to $(2.2 \pm 0.2) \times 10^{-7}$ M.

3.2 Molecular dynamic simulation experiments

Molecular Dynamics (MD) simulations were used to investigate the formation of HTyr-OL micelles, starting from a random

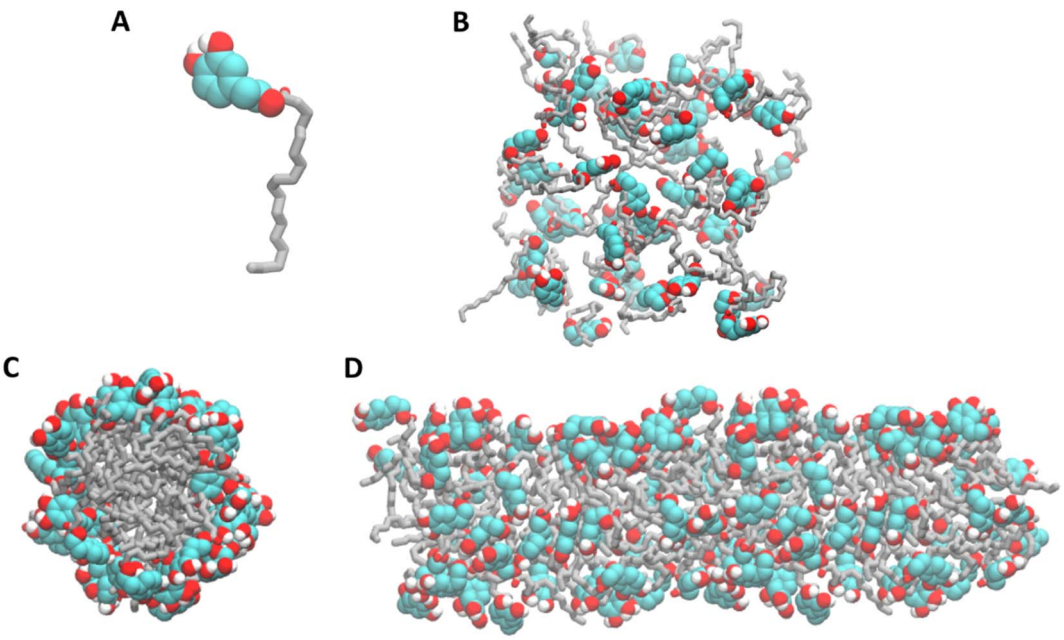

Fig. 2 (A) Structure of HTyr-OL. The carbon atoms of the HTyr head group are colored in turquoise whereas the carbon atoms of the acyl chain are colored in gray, and the oxygen atoms are colored in red. For clarity, only the hydrogen bound to oxygen atoms are represented. (B) Initial configuration of the simulated system. The water molecules are not represented for clarity. (C and D) Snapshot of aggregate of HTyr-OL at the end of 100 ns of molecular dynamics simulations.

orientation of the monomers. In the first 4 ns of the MD simulation, HTyr-OL molecules form a worm-like structure, with the alkyl chains oriented toward the inner region of the aggregate and the HTyr head group exposed on the surface of the aggregate. This worm-like aggregate remains stable for the following 96 ns of the MD simulation, suggesting that at concentrations above its cmc HTyr-OL tends to form micellar aggregates with a cylindrical shape rather than spherical micelles (Fig. 2).

3.3 Physicochemical characterization of liposomes

The development of liposomes as suitable delivery systems for HTyr or HTyr-OL, involved the preparation of several liposome formulations employing different lipids, both natural and synthetic (Chart 1).

Due to their different molecular features (Chart 1), HTyr was entrapped within the lipid bilayer by a passive loading, whilst HTyr-OL, owing to its amphiphilic nature, was incorporated into the lipid bilayer, thereby contributing to the formation of liposome vesicles (Fig. 3).

Liposomes were prepared according to the thin layer evaporation method combined with a freeze–thaw protocol to reduce their lamellarity, followed by an extrusion process to obtain vesicles of the desired dimensions (~100 nm).

For all liposomes under investigation, physicochemical characterization was performed determining the hydrodynamic diameter (D_h) and polydispersity index (PDI) by DLS measurements, assessing ζ-potential through ELS measurements, and analyzing Entrapment Efficiency (EE%) by UPLC analysis.

HTyr embedded liposomes were formulated with natural phospholipids having different alkyl chain lengths, such as DOPC, DPPC, or DMPC, in the presence of Chol. This latter features a tetracyclic ring system with an alkyl side-chain extended towards the hydrophobic liposome region and a hydroxyl group oriented at the polar/non-polar interface.[68] Chol was incorporated into the lipid bilayer to produce liposomes with a more compact and stable structure, due to its capacity of inducing a dense packing and increasing the orientation order of the phospholipid hydrocarbon chains.[69]

The results reported in the Table 1 evidenced a narrow size distribution for all liposomes, with diameters ranging from 119 to 137 nm and a good PDI (0.04–0.10), consistently with the extrusion protocol adopted during the preparation.

The investigation of the surface charge of the liposomes of formulations F1–F3 evidenced slightly negative ζ-potential values, compared to empty liposomes F1e–F3e, probably due to HTyr ability to interact with ester oxygens and phosphate groups through hydrogen bonds. The presence of HTyr at lipid–water interface and the interaction with polar head groups reduces the number of Na^+ ions associated to phosphate and ester groups, and induces a different orientation of phosphocholine portion of DOPC/DPPC/DMPC with respect to normal lipid bilayer.[70]

Regarding EE% values, all liposomes of formulations F1–F3 featured high entrapment efficiency, with no significant differences in the concentration of entrapped HTyr among the designed formulations.

Regarding HTyr-OL based liposomes, these were first formulated with a natural phospholipid (DOPC, DPPC, or DMPC), either in the presence or absence of Chol. Subsequently, in the perspective of promoting the interaction between the liposomes and the bacterial cells involved in our study, some formulations were prepared using DPPC as the natural phospholipid, in the presence of the synthetic cationic amphiphile LIPCAT (Chart 1), added at different molar ratios. LIPCAT inclusion into the lipid bilayer provides positively charged liposomes, thereby enhancing electrostatic interactions with bacterial cells, which typically exhibit a negative charge on their cell walls. Specifically, we decided to formulate HTyr-OL based cationic liposome employing DPPC and LIPCAT, following a previous study that demonstrates how DPPC/LIPCAT liposomes are particularly effective at interacting with *S. aureus*.[71]

According to the results in Table 2, HTyr-OL based liposomes showed dimensions ranging from 94 to 116 nm and suitable PDI values (0.04–0.14).

Regarding the vesicles surface charge, liposomes of formulations F4–F9 exhibited negative ζ-potential values, probably due to the exposure of the HTyr-OL catechol moiety on the liposomes surface, as well as the phosphocholine phosphate groups of the lipids DOPC, DPPC, or DMPC used in the formulation. Conversely, cationic liposomes of formulations

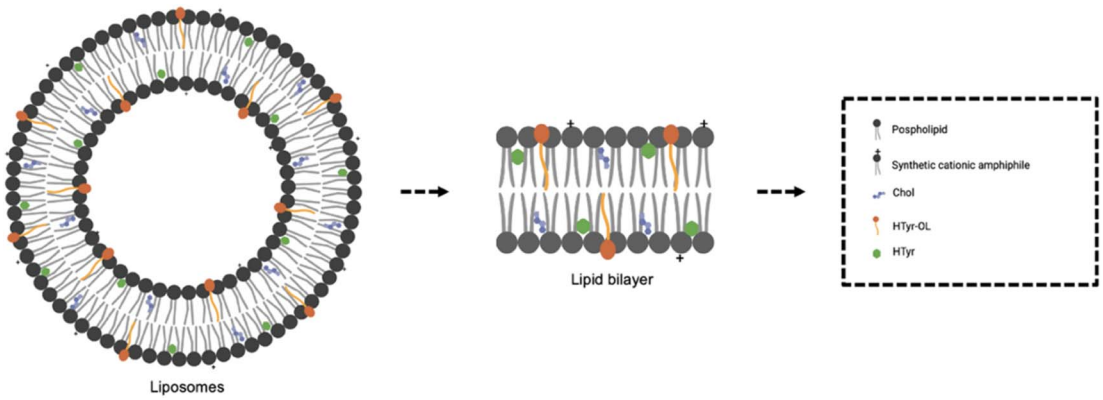

Fig. 3 Schematic drawing illustrating the proposed locations of all the components in the developed liposomes (created with bioRender.com).

Table 1 Physicochemical features of empty liposomes (10 mM in total lipids) and HTyr-loaded liposomes (20 mM in total lipids) in PBS (pH 7.4)

Formulation	Composition	D_h (nm)	PDI	ζ-potential (mV)	EE (%)	HTyr[c] (mM)
F1e[a]	DOPC/Chol 8.0:2.0	119 ± 2	0.10 ± 0.02	−3 ± 2	—	—
F1	DOPC/Chol/HTyr[b] 16.0:4.0:2.5	119 ± 1	0.08 ± 0.04	−8.7 ± 0.4	79 ± 6	1.68 ± 0.02
F2e[a]	DPPC/Chol 8.0:2.0	137 ± 1	0.05 ± 0.02	−5 ± 1	—	—
F2	DPPC/Chol/HTyr[b] 16.0:4.0:2.5	130 ± 1	0.04 ± 0.02	−6 ± 2	75 ± 4	1.68 ± 0.05
F3e[a]	DMPC/Chol 8.0:2.0	131 ± 1	0.044 ± 0.002	−4 ± 1	—	—
F3	DMPC/Chol/HTyr[b] 16.0:4.0:2.5	129 ± 1	0.09 ± 0.01	−5 ± 1	70 ± 3	1.67 ± 0.02

[a] Empty liposomes. [b] [HTyr]/[total lipids] molar ratio at the beginning of the preparation is 1/8. [c] HTyr concentration in liposomes determined by UPLC analysis.

F10 and F11 exploited quite high positive ζ-potential values, +42 mV and +29 mV, respectively, due to the presence of LIPCAT within the lipid bilayer.

Additionally, cationic reference liposomes, prepared in the absence of HTyr-OL, were formulated with DPPC and LIPCAT, added at different molar ratios, to estimate the potential contribution of LIPCAT on the biological activity of the liposomes under investigation. Both liposomes of formulations F10ref and F11ref displayed appropriate dimensions, good PDI values, and high positive ζ-potential values, as reported in Table 2.

The final concentration of HTyr-OL in liposomes of formulations F4–F11 was quantified by ^{1}H NMR analysis, which confirmed, approximatively, the molar concentration initially used for liposomes production. This analysis was particularly useful for the dosage of HTyr-OL, when loaded in liposomes, especially for assessing the antimicrobial experiments described below.

Finally, HTyr was entrapped in liposomes formulated with the natural phosphocholine DOPC in the presence of Chol, further functionalized through the inclusion of HTyr-OL into the lipid bilayer, with the aim to investigate the effect on the physicochemical and biological properties of the liposomes due to the simultaneous conveyance of both HTyr and HTyr-OL. In this case as well, liposomes of formulation F12 exhibited suitable dimensions, an excellent PDI, a negative ζ-potential, and high entrapment efficiency, with good final concentrations of both HTyr and HTyr-OL (Table 3).

3.3.1 Liposomes stability. The storage stability of liposomes F1–F12 was investigated over 28 days. Vesicles were

Table 2 Physicochemical features of HTyr-OL based liposomes (10 mM in total lipids) in PBS (pH 7.4)

Formulation	Composition	D_h (nm)	PDI	ζ-potential (mV)	HTyr-OL[a] (mM)
F4	DOPC/Chol/HTyr-OL 7.0:2.0:1.0	116 ± 2	0.14 ± 0.01	−3.0 ± 0.2	0.94 ± 0.09
F5	DOPC/HTyr-OL 8.0:2.0	95 ± 3	0.13 ± 0.01	−8 ± 3	1.56 ± 0.04
F6	DPPC/Chol/HTyr-OL 7.0:2.0:1.0	110 ± 3	0.08 ± 0.01	−8 ± 2	1.02 ± 0.05
F7	DPPC/HTyr-OL 8.0:2.0	104 ± 3	0.06 ± 0.01	−17 ± 1	1.89 ± 0.07
F8	DMPC/Chol/HTyr-OL 7.0:2.0:1.0	119 ± 4	0.06 ± 0.01	−14 ± 2	0.84 ± 0.05
F9	DMPC/HTyr-OL 8.0:2.0	96 ± 2	0.08 ± 0.02	−14 ± 2	1.95 ± 0.03
F10	DPPC/LIPCAT/HTyr-OL 7.0:2.0:1.0	94 ± 1	0.04 ± 0.01	42 ± 2	1.41 ± 0.06
F11	DPPC/HTyr-OL/LIPCAT 7.0:2.0:1.0	95 ± 1	0.11 ± 0.01	29 ± 2	1.71 ± 0.07
F10ref	DPPC/LIPCAT 8.0:2.0	108 ± 1	0.04 ± 0.02	37 ± 2	—
F11ref	DPPC/LIPCAT 9.0:1.0	102 ± 1	0.08 ± 0.02	26 ± 1	—

[a] HTyr-OL quantification in liposomes determined by ^{1}H NMR analysis.

Table 3 Physicochemical features of HTyr loaded liposomes functionalized with HTyr-OL (10 mM in total lipids) in PBS (pH 7.4)

Formulation	Composition	D_h (nm)	PDI	ζ-potential (mV)	EE (%)	HTyr[b] (mM)	HTyr-OL[c] (mM)
F12	DOPC/Chol/HTyr-OL/HTyr[a] 7.0:2.0:1.0:1.25	111 ± 1	0.08 ± 0.01	−7 ± 3	76 ± 3	0.85 ± 0.02	0.91 ± 0.07

[a] [HTyr]/[total lipids] molar ratio at the beginning of the preparation is 1/8. [b] HTyr concentration in liposomes determined by UPLC analysis. [c] HTyr-OL quantification in liposomes determined by ^{1}H NMR analysis.

maintained at 4 °C, protected from light, and determination of particles diameter and PDI values were performed by DLS analysis.

The data reported in Table S1† displayed excellent stability under these storage conditions for liposomes of formulations F1–F10 and F12, while liposomes of formulation F11 exhibited an increase in dimensions and PDI starting from the first week of storage. Specifically, the presence of a second and third population was observed, with dimensions around 1000 and 5000 nm, respectively, evidencing an unexpected physical instability for liposome of formulation F11 due to aggregation phenomena (Fig. 4).

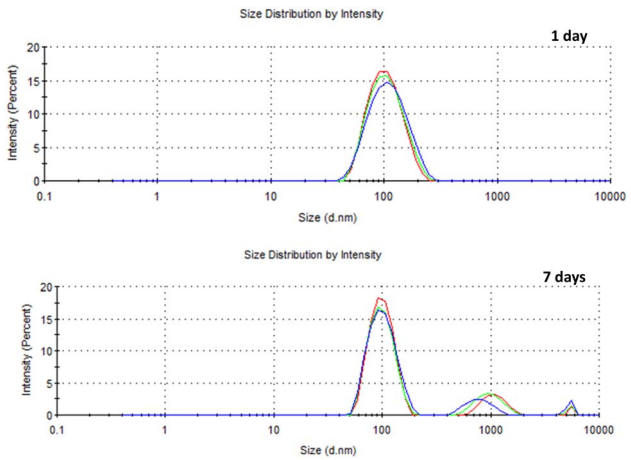

Fig. 4 Variation in the size distribution of formulation F11 over time. The three differently colored curves (red, green and blue) represent distinct measurements obtained from the same sample of formulation F11.

In the perspective of a potential *in vivo* oral administration, liposomes may undergo significant pH variations, which could represent an environmental shock condition that affects the positioning of HTyr or HTyr-OL within the lipid bilayer[72] and potentially induce liposomes degradation or aggregation.

Therefore, the pH stability of HTyr (F1–F3) and HTyr-OL (F4, F6, F8 and F12) loaded liposomes was evaluated by monitoring vesicles size and PDI through DLS measurements at different pH values, mimicking those of the human digestive system and aligning with the physiological transit time. Data collected at different pH values (Table S2†) were compared to those obtained at pH 7.4 (reference value, data reported in blue), which corresponds to the physiological pH of blood.

All the liposomes of formulations under investigation exhibited excellent stability to pH variation, with no significant changes in either vesicle dimensions or PDI values.

3.3.2 *In vitro* release of HTyr from liposomes. The release profile of HTyr from liposomes of formulations F1–F3 and F12 was determined using a dialysis method. Specifically, the

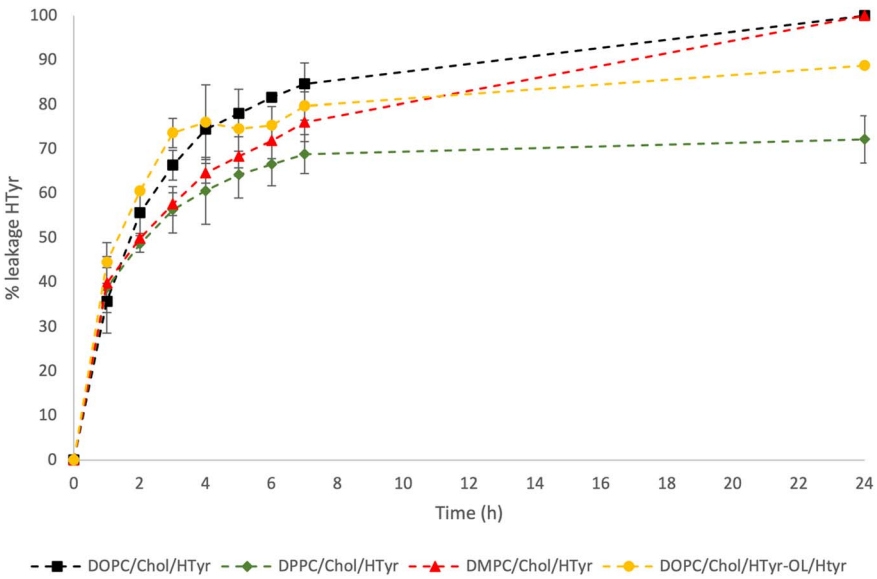

Fig. 5 HTyr forced released from liposomes of formulations F1 (black square), F2 (green rhombus), F3 (red triangles) and F12 (yellow dots).

leakage of HTyr from liposomes was monitored over a period of 24 h under forced release conditions, and the collected aliquots were analyzed by UPLC.

Fig. 5 illustrates the percentage of HTyr leakage from liposomes at specific time intervals. A similar trend was observed for all the developed liposome formulations, with approximately 50% of the entrapped HTyr being released within the first 2–4 h, followed by a gradual and slower release over the next 24 h. Notably, for liposomes of formulations F1 and F12, formulated with DOPC as the natural phospholipid, faster release profiles were detected, particularly within the first 7 h. A final HTyr releases of approximately 100% for liposomes F1 and 90% for liposomes F12 was observed after 24 h. Furthermore, liposomes formulated with DOPC and Chol in the presence of HTyr-OL, exhibited the highest HTyr release during the first 5 h, with approximately 80% HTyr leakage, compared to the other formulations.

Despite the slower release profile of HTyr from liposomes F3 formulated with DMPC and Chol, compared to F1 and F12, a final leakage of approximately 100% was observed. In contrast, for liposomes of formulation F2 composed of DPPC and Chol, a final leakage of about 70% was observed.

These findings may be attributed to the different membrane fluidity of the developed liposomes, which is influenced by the T_m of the main lipid involved in the preparation of the lipid bilayer: DOPC ($T_m \sim -16.5$ °C) < DMPC ($T_m \sim 23.6$ °C) < DPPC ($T_m \sim 41.4$ °C).

3.4 *In vitro* antimicrobial activity

The antimicrobial activity of HTyr and HTyr-OL, in free form and entrapped in liposomes, was investigated against two strains of *Staphylococcus aureus*, ATCC 25923 (wild type strain) and ATCC 33591 (MRSA, Methicillin-resistant *S. aureus*), to determine the Minimum Inhibitory Concentration (MIC) and the Minimum Bactericidal Concentration (MBC) according to the microdilution test procedure.

Firstly, HTyr and HTyr-OL were tested in free form against both bacterial strains under investigation; the obtained MIC and MBC values are expressed in Table 4 as μg mL^{-1} of compound and as absolute concentration (μM).

Based on the results expressed as absolute concentration, the antimicrobial effect exerted by HTyr-OL resulted higher than that showed by HTyr against both bacterial strains. In this perspective, the increased activity displayed by HTyr-OL could be related to its high lipophilic character, which may improve its passage through bacterial membranes, finally contributing to the improvement of its biological functionality.[73] Furthermore, HTyr-OL exhibited greater antimicrobial activity against ATCC 25923 (*S. aureus* wild type strain, MIC = 74 μM and MBC = 100 μM) compared to ATCC 33591 (MRSA strain, MIC = 99 μM and MBC = 116 μM).

Afterwards, the microdilution test was performed to evaluate the effect of liposome encapsulation on the antimicrobial activity of HTyr; the collected MIC and MBC values are expressed as absolute concentration (μM), as reported in Table 5.

Liposomes of formulation F1 exhibited a bactericidal effect against both tested bacteria, with slightly higher activity against ATCC 33591 (MBC value = 215 μM) compared to ATCC 25923 (MBC value = 235 μM). Regarding the inhibitory effect, we were not able to determine any MIC values for liposomes of formulation F1. However, we identified a concentration range within which the MIC values for both *S. aureus* strains are likely to fall, corresponding to 212–234 μM for ATCC 25923 and 194–214 μM for ATCC 33591.

The higher MIC and MBC values observed by testing HTyr loaded in DOPC/Chol liposomes (F1) should not be considered negative results, given the improvement in its pharmacokinetic features such as stability, bioavailability, releasing profile, *etc.*

Conversely, liposomes of formulations F2 and F3 did not exhibit any antimicrobial effect on *S. aureus* wild type and MRSA, even at the highest concentration tested in our

Table 4 Antimicrobial activity of HTyr and HTyr-OL against ATCC 25923 and ATCC 33591

	S. aureus wild type (ATCC 25923)				MRSA (ATCC 33591)			
Compound	MIC (μg mL^{-1})	MIC (μM)	MBC (μg mL^{-1})	MBC (μM)	MIC (μg mL^{-1})	MIC (μM)	MBC (μg mL^{-1})	MBC (μM)
HTyr	18	117	20	130	19	123	21	136
HTyr-OL	31	74	42	100	42	99	49	116

Table 5 Antimicrobial activity of HTyr free or loaded liposomes against ATCC 25923 and ATCC 33591[a]

		S. aureus wild type (ATCC 25923)		MRSA (ATCC 33591)	
Compound	Formulation	MIC (μM)	MBC (μM)	MIC (μM)	MBC (μM)
HTyr	—	117	130	123	136
	F1	n.d.	235	n.d.	215
	F2	n.a.	n.a.	n.a.	n.a.
	F3	n.a.	n.a.	n.a.	n.a.

[a] — = HTyr in free form; n.d. = not determined; n.a. = no activity.

experimental conditions. This evidence may be related to the slower release profile of HTyr from liposomes composed by DPPC/Chol and DMPC/Chol (Fig. 3), which is closely related to their lower membrane fluidity[74–76] compared to DOPC/Chol based liposomes, thereby affecting the release of the encapsulated compound.

The antimicrobial activity of HTyr-OL was also investigated after its entrapment in liposomes. To assess the dosage of HTyr-OL in liposomes for the antimicrobial experiments, ^{1}H NMR analyses were performed as previously described. It is important to note that, due to its amphiphilic nature, HTyr-OL within the lipid bilayer is oriented toward both the aqueous core of the liposomes and the surrounding aqueous medium at the external lipid bilayer–water interface (Fig. 3). Consequently, since HTyr-OL as a component of the lipid bilayer is not released from liposomes, we attribute any potential antimicrobial activity solely to HTyr-OL molecules oriented toward the surrounding aqueous medium at the external lipid bilayer–water interface. Therefore, the concentration of HTyr-OL tested in the liposomes is theoretically half of the initially dosed amount.

Liposomes of formulations F4–F9 did not display any antimicrobial effect against either bacterial strain. As a result, it was not possible to determine MIC and MBC values (Table 6), even though the highest testable amount of HTyr-OL embedded within the lipid bilayers was tested under our experimental conditions.

The antimicrobial activity of cationic liposome formulations F10–F11, containing different molar ratios of the cationic lipid LIPCAT and HTyr-OL, was evaluated to determine whether the lack of activity observed for formulations F4–F9 was due to the absence of electrostatic interactions between neutral liposomes and the bacterial strains studied. In this regard, as previously mentioned, the literature reports that DPPC/LIPCAT liposomes are particularly effective in interacting with *S. aureus* bacteria.[71]

According to the results reported in Table 6, antimicrobial activity was observed for both cationic formulations F10 and F11, but some important considerations must be made.

Although HTyr-OL in liposomes F10 demonstrated activity against both *S. aureus* wild type and MRSA (MBC value = 58 μM on both strains), this effect was influenced by the high concentration of LIPCAT in liposomes of formulation F10, which amounted to 107 μM. In fact, the same antimicrobial activity was observed for liposomes of formulation F10ref, which contained the same amount of LIPCAT as liposomes of formulation F10 but without HTyr-OL (see Table 2). This suggests that the observed effect can be attributed to the presence of LIPCAT within the lipid bilayer, rather than to the entrapped HTyr-OL.

Liposomes of formulation F11ref, which lacked HTyr-OL and were formulated with half the molar ratio of LIPCAT compared to liposomes of formulation F10 (see Table 2), exploited no antimicrobial effect against either bacterial strain. Consequently, the antimicrobial activity observed for cationic liposomes of formulation F11, containing the same amount of LIPCAT as F11ref, can be attributed exclusively to the presence of HTyr-OL. Specifically, liposomes of formulation F11 showed an inhibitory effect only on MRSA growth (MIC value = 271 μM), with no bactericidal effect against MRSA, and any kind of activity against *S. aureus* wild type strain.

However, the inhibitory effect observed on MRSA after treatment with liposomes of formulation F11 was not completely reproducible, because half of the assessed antimicrobial tests showed no effect on MRSA growth. These

Table 6 Antimicrobial activity of HTyr-OL free or embedded in liposomes against ATCC 25923 and ATCC 33591[a]

		S. aureus wild type (ATCC 25923)		MRSA (ATCC 33591)	
Compound	Formulation	MIC (μM)	MBC (μM)	MIC (μM)	MBC (μM)
	—	74	100	99	116
HTyr-OL	F4	n.a.	n.a.	n.a.	n.a.
	F5	n.a.	n.a.	n.a.	n.a.
	F6	n.a.	n.a.	n.a.	n.a.
	F7	n.a.	n.a.	n.a.	n.a.
	F8	n.a.	n.a.	n.a.	n.a.
	F9	n.a.	n.a.	n.a.	n.a.
	F10	n.d.	58	n.d.	58
	F11	n.a.	n.a.	271	n.d.

[a] — = HTyr-OL in free form; n.d. = not determined; n.a. = no activity.

Table 7 Antimicrobial activity of HTyr entrapped in liposomes functionalized with HTyr-OL against ATCC 25923 and ATCC 33591[a]

		S. aureus wild type (ATCC 25923)		MRSA (ATCC 33591)	
Compound	Formulation	MIC (μM)	MBC (μM)	MIC (μM)	MBC (μM)
HTyr	—	117	130	123	136
	F12	n.d.	174	n.d.	191

[a] — = HTyr in free form; n.d. = not determined.

inconsistent results are probably due to the instability of liposomes of formulation F11, which, as previously discussed (see Table S1†), are not completely stable over time. Therefore, the inhibitory effect noted in some instances against MRSA might be attributed to the activity of HTyr-OL released from the liposomes after their aggregation over time.

Finally, the antimicrobial activity of HTyr loaded in liposomes functionalized with HTyr-OL was evaluated against ATCC 25923 and ATCC 33591 strains, examining the simultaneous conveyance of HTyr both in its original form and as the acyl derivative.

Liposomes of formulation F12 exhibited a bactericidal effect against both tested bacteria, with slightly higher activity against the wild type strain (ATCC 25923, MBC value = 174 μM) compared to MRSA (ATCC 33591, MBC value = 191 μM), as reported in Table 7. Regarding the inhibitory effect, no MIC values were determined for either tested strain under our experimental conditions. However, we identified a concentration range within which the MIC values for both *S. aureus* strains are likely to fall, corresponding to 137–173 μM for ATCC 25923 and 154–190 μM for ATCC 33591.

When comparing the activity of HTyr in its free form and after loading in liposomes (in particular in formulations F1 and F12), HTyr in liposomes F12 displayed an intermediate activity between HTyr tested in free form and HTyr loaded in liposomes F1. This effect is likely due to the presence of HTyr-OL in liposomes of formulation F12, which is absent in those of formulation F1. The inclusion of HTyr-OL in the DOPC/Chol lipid bilayer may influence the localization of HTyr toward the liposome surface rather than the inner region, due to the mutual affinity between the catechol groups of HTyr and HTyr-OL. Indeed, as shown in Fig. 5, a faster release profile of HTyr from liposomes F12 was observed compared to liposomes F1, particularly during the first 3 h.

3.5 Hydrogen atom transfer reactions

In order to investigate the effect of the chemical modification of HTyr to HTyr-OL on its antioxidant properties, the antioxidant activity of HTyr and HTyr-OL in their free forms was assessed by analysing their reactivity in hydrogen atom transfer (HAT) reactions, promoted by galvinoxyl (GO$^{\bullet}$) and 2,2-diphenylpycrylhydrazyl (DPPH$^{\bullet}$) radicals (Scheme 1).

The rate constants for HAT (k_H) from HTyr and HTyr-OL to GO$^{\bullet}$ and DPPH$^{\bullet}$ were determined spectrophotometrically in CH_3CN by monitoring the decay of the radicals' corresponding visible absorption bands, at 428 and 517 nm, respectively.

CH_3CN was chosen to carry out the HAT kinetics experiment because in polar protic solvents (*e.g.* ethanol or methanol; GO$^{\bullet}$ and DPPH$^{\bullet}$ are insoluble in water) the reaction between DPPH$^{\bullet}$ and phenols is strongly accelerated by a stepwise proton-transfer electron-transfer mechanism (known as SPLET).[77]

Clean first-order decays (k_{obs}) were observed, and linear dependencies of k_{obs} on the concentration of the phenols were obtained (Fig. 6).

From the slopes of these plots, the k_H values were determined. All kinetic data for HAT from HTyr and HTyr-OL promoted by GO$^{\bullet}$ and DPPH$^{\bullet}$ are reported in Table 8. The kinetic constants measured for HTyr and HTyr-OL indicate a comparable and notable reactivity of both phenolic compounds toward each radical investigated.

HAT reactions from various phenols have been extensively investigated in the literature[78,79] due to their involvement in several biological and chemical phenomena. The determination of the hydrogen atom transfer rate constant, k_H, is a useful key element for evaluating the performance of phenols as antioxidants. It generally depends on the bond dissociation enthalpy (BDE) of the phenolic O–H bond, as well as the steric hindrance around the phenolic group. Electron-donating (ED) groups lower the BDE(O–H) while electron-withdrawing (EW) groups have the opposite effect; this mainly depends on their ability to stabilize the phenoxyl radical formed after H-atom abstraction.[79]

In catecholic compounds, such as HTyr and HTyr-OL, the presence of an *ortho* –OH group on the aromatic ring, not only lowers the phenolic BDE(O–H) but also stabilizes both the phenol and, to a greater extent, the phenoxyl radical produced. This structural feature confers significant antioxidant activity to these compounds.[80]

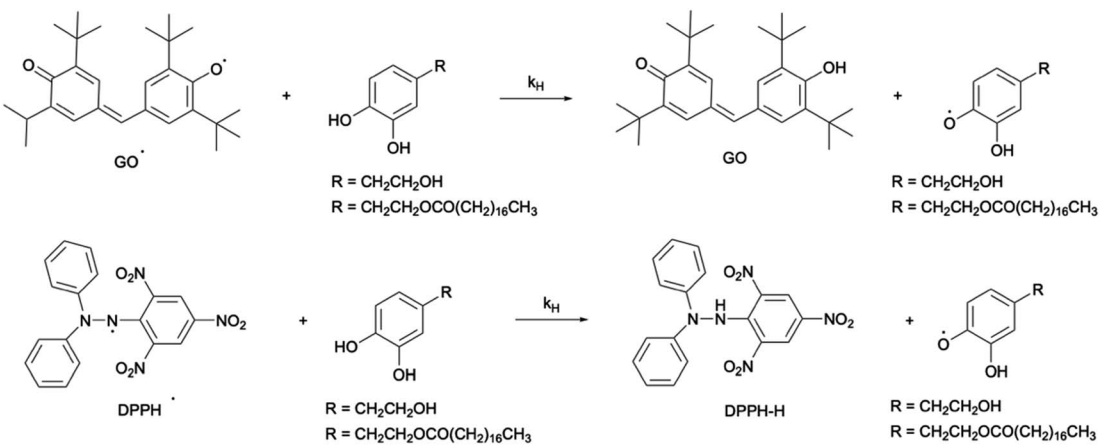

Scheme 1 Hydrogen atom transfer reaction from phenols to GO$^{\bullet}$ and DPPH$^{\bullet}$.

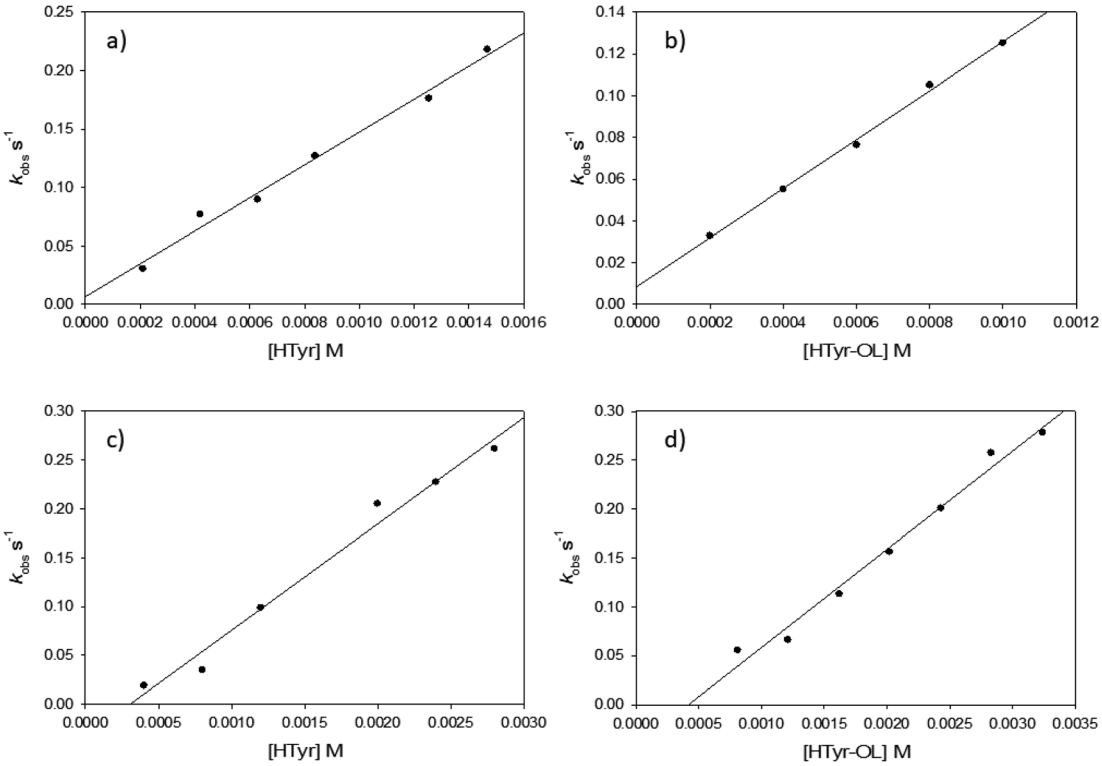

Fig. 6 Plot of the observed rate constant (k_{obs}) against [HTyr] and [HTyr-OL] for the reaction with GO$^{\bullet}$ (a and b) and with DPPH$^{\bullet}$ (c and d) measured in CH_3CN at 25 °C. k_{obs} values were obtained following the decay of GO$^{\bullet}$ and of DPPH$^{\bullet}$ at 428 and 517 nm, respectively.

In fact, both compounds show k_H values similar to those of other potent antioxidant phenolic compounds,[81] for example k_H from α-Tocopherol to DPPH$^{\bullet}$ is 490 M^{-1} s^{-1}.[82]

In particular, HTyr is marginally more reactive than HTyr-OL with both radicals, the k_H values collected for HTyr are slightly higher than those obtained with HTyr-OL. This is because GO$^{\bullet}$ and DPPH$^{\bullet}$ are characterized by significant steric hindrance protecting the radical center, and since HTyr-OL, unlike HTyr, is characterized by the presence of a long alkyl chain, this can make the hydrogen atom transfer process slightly less favorable.

3.6 Evaluation of active catechol residues in HTyr-OL based liposomes against ABTS$^{\bullet+}$

The antioxidant activity of HTyr and HTyr-OL is related to the catechol group in their molecular structure. To evaluate whether this antioxidant capacity was preserved in HTyr-OL based liposomes of formulations F4, F6 and F8, where the catechol residues are exposed on the external liposomal surface, reactions between ABTS$^{\bullet+}$ and either HTyr-OL or HTyr-OL based liposomes were carried out in buffered water at 25 °C.

ABTS$^{\bullet+}$ is a colored and relatively persistent radical cation that exhibits a strong absorption band at 734 nm. Unlike GO$^{\bullet}$, DPPH$^{\bullet}$, and other organic radical species, which are only soluble in organic solvents, ABTS$^{\bullet+}$ is water soluble and can be generated in buffered water. These experimental conditions are perfectly compatible with our liposomal formulations, which would not withstand organic solvents.

The amount of ABTS$^{\bullet+}$ quenched after 10 min (fixed time point) by liposomes of formulations F4, F6, and F8 was compared to that produced by HTyr-OL in its free form, allowing for the determination of the concentration (mM) of active catechol residues exposed on the external liposomal surface.

In Table 9 the concentration (mM) of active catechol residues is reported for each formulation, along with the total amount of HTyr-OL, determined by ^{1}H-NMR measurement, effectively present in the liposomal suspension and the percentage of HTyr-OL active residues exposed on the external surface of liposomes under investigation.

Taking into account that only half of the total amount of HTyr-OL molecules in liposomes F4, F6 and F8 are located in the external lipid layer and can expose their catechol residues toward the external lipid bilayer–water interface, it is noteworthy that liposomes of formulation F4 exhibited the highest concentration of active catechol residues on their surface, compared to those of formulations F6 and F8, likely corresponding to their entirety. This suggests that liposomes of

Table 8 Second order rate constants k_H (M^{-1} s^{-1}) for HAT reaction from HTyr and HTyr-OL to GO$^{\bullet}$ and DPPH$^{\bullet}$ measured at 25 °C

	k_H (M^{-1} s^{-1})	
Radical	HTyr	HTyr-OL
GO$^{\bullet}$	137 ± 4	119 ± 2
DPPH$^{\bullet}$	115 ± 8	108 ± 10

Table 9 Total amount of HTyr-OL in liposomes, concentration of HTyr-OL active catechol residues and % of HTyr-OL active catechol residues exposed on the external surface of liposomes of formulations F4, F6, and F8

Formulation	Composition	HTyr-OL (mM)	HTyr-OL active residues (mM)	HTyr-OL active residues (%)
F4	DOPC/Chol/HTyr-OL	0.94 ± 0.09	0.4 ± 0.1	88 ± 6
F6	DPPC/Chol/HTyr-OL	1.02 ± 0.05	0.29 ± 0.05	48 ± 10
F8	DMPC/Chol/HTyr-OL	0.84 ± 0.05	0.27 ± 0.01	58 ± 8

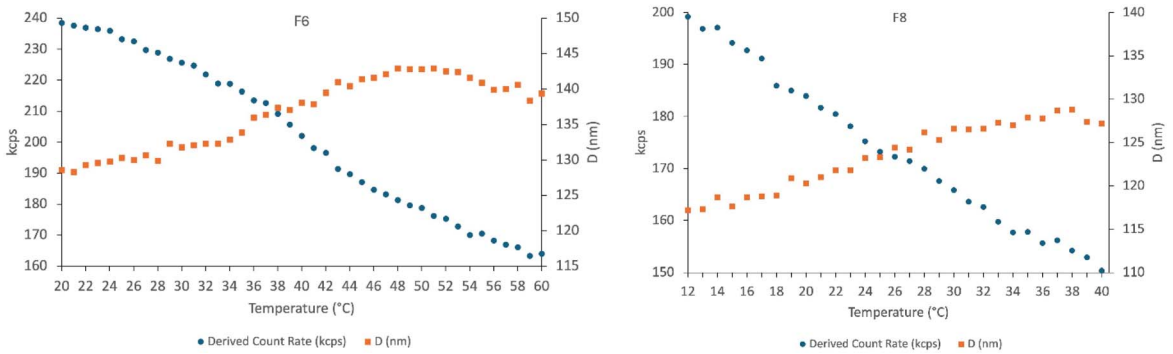

Fig. 7 Variation in derived count rate (k_{cps}, blu dots) and particle diameter (D, orange square) measured as a function of temperature for liposomes of formulations F6 (DPPC/Chol/HTyr-OL) and F8 (DMPC/Chol/HTyr-OL).

formulations F4 may exhibit greater antioxidant activity than those of formulations F6 and F8.

These results may be related to differences in membrane fluidity of the developed liposomes. Liposomes of formulation F4, which are primarily composed of DOPC, likely exhibit greater membrane fluidity at 25 °C than those of formulations F6 and F8. As a result, the catechol residues exposed on their external surface could be more accessible and properly oriented to react with $ABTS^{\bullet+}$.

To confirm this, DLS was chosen as the technique to investigate the membrane fluidity of liposomes F4, F6 and F8. This method evaluates changes in the optical properties of lipids in liposomes by assessing variations in the mean count rate and vesicles size with increasing temperature. In fact, changes in these two parameters are related to modifications inside the membrane structure, and the typical trend observed is opposite: the count rate decreases while the particles size increases.[62]

Fig. 7 shows the derived count rate (k_{cps}) and the vesicles diameter (D) measured for liposomes of formulations F6 and F8 at increasing temperature. In both cases, a clear transition was not observed, as it occurred gradually within the temperature range investigated.

Although the addition of Chol and HTyr-OL increased the complexity of the developed bilayers, liposomes of formulations F6 (DPPC/Chol/HTyr-OL) and F8 (DMPC/Chol/HTyr-OL) exhibited transition temperatures (T_m) quite close to that of the main lipid component, approximately 41.4 °C for DPPC and 23.6 °C for DMPC, as reported in the literature.[62–64] Therefore, it can be concluded that the presence of Chol and HTyr-OL as minor components within the lipid bilayers of the investigated liposomes does not significantly affect their membrane fluidity.

Similar considerations can be applied to liposomes of formulation F4 (DOPC/Chol/HTyr-OL), for which the experiment was not conducted due to the very low transition temperature of its main lipid component, DOPC with a T_m of approximately – 16.5 °C, as reported in the literature.[83]

These results confirm that at 25 °C, the membrane of liposomes F4 is characterized by a more fluidity than those of liposomes F6 and F8, allowing the catechol residues to be more responsive in reacting with $ABTS^{\bullet+}$.

4. Conclusion

In conclusion, the high lipophilic character of HTyr-OL results in a stronger antimicrobial effect compared to HTyr against both tested strains of *Staphylococcus aureus*: ATCC 25923 (wild type strain) and ATCC 33592 (MRSA).

Experimental data concerning antioxidant activity of HTyr and HTyr-OL, determined by measuring the kinetic rate constants of the hydrogen atom transfer reactions to two different radicals, $GO^{\bullet}$ and $DPPH^{\bullet}$, demonstrated significant and comparable activity for both phenolic compounds against each radical investigated, due to the reactivity of the catecholic residue in their molecular structures.

Therefore, the chemical modification of HTyr in HTyr-OL does not affect the antioxidant activity whereas its antimicrobial activity against *S. aureus* is increased.

Conversely, the encapsulation of HTyr in liposomes, formulated with natural and synthetic amphiphiles, has not led to any improvement in its antimicrobial activity. However, the higher MIC and MBC values observed for HTyr loaded in DOPC/Chol based liposomes (F1 and F12) are nonetheless

encouraging, especially given the enhancement in HTyr pharmacokinetic features such as stability, bioavailability, releasing profile, *etc.*

Although no antimicrobial activity has been observed for HTyr-OL based liposomes against the investigated *S. aureus* strains, we found that the significant antioxidant activity of HTyr-OL was preserved when added as a component of the lipid bilayer in liposomes.

This finding is particularly noteworthy, as HTyr-OL based liposomes may represent a promising tool for treating various diseases where oxidative stress plays a major role in damaging biological systems[84,85] including the aging process,[86,87] atherosclerosis and ischemic heart disease,[88] rheumatoid arthritis,[89] cancer,[90] pulmonary infections,[91,92] and brain ischemia.[93]

Data availability

The data supporting this article have been included as part of the ESI.†

Author contributions

Giuliana Prevete: conceptualization, data curation, formal analysis, investigation, methodology, validation, visualization, writing – original draft preparation; Elisa Sciopioni: investigation, formal analysis; Enrica Donati: conceptualization, formal analysis, investigation, methodology, validation, writing – review & editing; Noemi Villanova: investigation, methodology, writing – review & editing; Andrea Fochetti: investigation, methodology, writing – review & editing; Laura Lilla: formal analysis, investigation; Stefano Borocci: data curation, formal analysis, investigation, methodology, validation, writing – review & editing; Roberta Bernini: conceptualization, funding acquisition, methodology, resources, writing – original draft preparation; Marco Mazzonna: conceptualization, data curation, formal analysis, funding acquisition, methodology, project administration, resources, supervision, visualization, writing – original draft preparation.

Conflicts of interest

There are no conflicts to declare.

Acknowledgements

The authors are grateful to Innovation Ecosystem Rome Technopole, National Recovery and Resilience Plan (NRRP), Mission 4, Component 2 Investment 1.5, funded from the European Union-Next Generation EU (Code Project: ECS00000024) and to the DAFNE Project Departments of Excellence "Digital, Intelligent, Green and Sustainable" (D.I.Ver.So) granted by MUR (2023–2027). Moreover, this research was partially funded by the following projects: "One Health Basic and Translation Research Actions addressing unmet Needs on Emerging Infectious Diseases, INF-ACT" NRRP Next Generation EU project (Project code PE00000007); CNR project FOE-2021 NUTRAGE DBA.AD005.225; "ON Foods-Research and innovation network on food and nutrition Sustainability, Safety and Security—Working ON Foods" NRRP Next Generation EU project (Project code PE00000003).

References

1 R. W. Owen, A. Giacosa, W. E. Hull, R. Haubner, G. Würtele, B. Spiegelhalder and H. Bartsch, *Lancet Oncol.*, 2000, **1**(2), 107.
2 E. Tripoli, M. Giammanco, G. Tabacchi, D. Di Majo, S. Giammanco and M. La Guardia, *Nutr. Res. Rev.*, 2005, **18**(1), 98.
3 G. Prevete, E. Donati, A. P. Ruggiero, S. Fardellotti, L. Lilla, V. Ramundi, I. Nicoletti, F. Mariani and M. Mazzonna, *ACS Appl. Mater. Interfaces*, 2024, **16**(50), 68850.
4 G. Prevete, L. G. Carvalho, M. Del Carmen Razola-Diaz, V. Verardo, G. Mancini, A. Fiore and M. Mazzonna, *Ultrason. Sonochem.*, 2024, **102**, 106765.
5 T. Sar and M. Y. Akbas, *Sustainability*, 2023, **15**, 8179.
6 A. Hernandez-Fernandez, Y. Garrido, E. Iniesta-Lopez, J. Quesada-Medina and F. J. Hernandez-Fernandez, *Processes*, 2023, **11**, 2668.
7 M. Robles-Almazan, M. Pulido-Moran, J. Moreno-Fernandez, C. Ramirez-Tortosa, C. Rodriguez-Garcia, J. L. Quiles and M. C. Ramirez-Tortosa, *Food Res. Int.*, 2018, **105**, 654.
8 S. Charoenprasert and A. Mitchell, *J. Agric. Food Chem.*, 2012, **60**(29), 7081.
9 M. C. L. De las Hazas, L. Rubio, A. Macia and M. Motilva, *Pharm. Des.*, 2018, **24**, 2157.
10 M. Bertelli, A. K. Kiani, S. Paolacci, E. Manara, D. Kurti, K. Dhuli, V. Bushati, J. Miertus, D. Pangallo, M. Baglivo, T. Beccari and S. Michelini, *J. Biotechnol.*, 2020, **309**, 29.
11 M. C. L. De las Hazas, L. Rubio, A. Macia and M. J. Motilva, *Curr. Pharm. Des.*, 2018, **24**, 2157.
12 J. Rodriguez-Morato, L. Xicota, M. Fito, M. Farre, M. Dierssen and R. de la Torre, *Molecules*, 2015, **20**, 4655.
13 A. Boronat, G. Serreli, J. Rodriguez-Morat, M. Deiana and R. de la Torre, *Antioxidants*, 2023, **12**, 1472.
14 L. Micheli, L. Bertini, A. Bonato, N. Villanova, C. Caruso, M. Caruso, R. Bernini and F. Tirone, *Nutrients*, 2023, **15**(7), 1767.
15 R. Fabiani, M. V. Sepporta, P. Rosignoli, A. De Bartolomeo, M. Crescimanno and G. Morozzi, *Eur. J. Nutr.*, 2012, **51**, 455.
16 S. Li, H. Shao, T. Sun, X. Guo, X. Zhang, Q. Zeng, S. Fang, X. Liu, F. Wang, F. Liu and P. Ling, *Front. Pharmacol*, 2024, **15**, 1366683.
17 R. Bernini, M. S. Gilardini Montani, N. Merendino, A. Romani and F. Velotti, *J. Med. Chem.*, 2015, **58**, 9089.
18 L. Parkinson and S. Cicerale, *Molecules*, 2016, **21**, 1734.
19 J. S. Perona, R. Cabello-Moruno and V. Ruiz-Gutierrez, *J. Nutr. Biochem.*, 2006, **17**, 429.
20 W. A. Batarfi, M. H. M. Yunus, A. A. Hamid, Y. T. Lee and M. Maarof, *Pharmaceutics*, 2024, **16**, 1504.
21 H. Jemai, A. El Feki and S. Sayadi, *J. Agric. Food Chem.*, 2009, **57**, 8798.
22 R. Capasso, A. Evidente, S. Avolio and F. Solla, *J. Agric. Food Chem.*, 1999, **47**(4), 1745.

23 A. Malapert, E. Reboul, O. Dangles, A. Thiéry, N. Sylla and V. Tomao, *Molecules*, 2021, **26**, 4463.
24 M. Bellumori, L. Cecchi, A. Romani, N. Mulinacci and M. Innocenti, *J. Sci. Food Agric.*, 2018, **98**, 2761.
25 R. Bernini, M. Campo, C. Cassiani, A. Fochetti, F. Ieri, A. Lombardi, S. Urciuoli, P. Vignolini, N. Villanova and C. Vita, *J. Agric. Food Chem.*, 2024, **72**, 12871.
26 M. Robles-Almazan, M. Pulido-Moran, J. Moreno-Fernandez, C. Ramirez-Tortosa, C. Rodriguez-Garcia, J. L. Quiles and M. C. Ramirez-Tortosa, *Food Res. Int.*, 2018, **105**, 654.
27 M. Navarro and F. J. Morales, *Food Chem.*, 2017, **217**, 602.
28 G. Corona, D. Vauzour, A. Amini and J. P. E. Spencer, in *Polyphenols in Human Health and Disease*, ed. R. Ross Watson, V. R. Preedy and S. Zibadi, Academic Press, 2014, vol. 44, p. 591.
29 M. González-Santiago, J. Fonollá and E. Lopez-Huertas, *Pharm. Res.*, 2010, **61**(4), 364.
30 C. Bender, S. Strassmann and C. Golz, *Nutrients*, 2023, **15**, 325.
31 B. Hu, X. Liu, C. Zhang and X. Zeng, *J. Food Drug Anal.*, 2017, **25**(1), 3.
32 S. Gao and M. Hu, *Mini Rev. Med. Chem.*, 2010, **10**(6), 550.
33 R. Mateos, G. Pereira-Caro, S. Saha, R. Cert, M. Redondo-Horcajo, L. Bravo and P. A. Kroon, *Food Chem.*, 2011, **125**(3), 865.
34 D. Tofani, V. Balducci, T. Gasperi, S. Incerpi and A. Gambacorta, *J. Agric. Food Chem.*, 2010, **58**(9), 5292.
35 G. Fernandez-Bolanos, O. Lopez, J. Fernandez-Bolanos and G. Rodriguez-Gutierrez, *Curr. Org. Chem.*, 2008, **12**(6), 442.
36 J. G. Fernandez-Bolanos, O. Lopez, M. A. Lopez-Garcia and A. Marset, *Biological Properties of Hydroxytyrosol and Its Derivatives*, InTech, 2012, p. 375.
37 R. Bernini, I. Carastro, F. Santoni and M. Clemente, *Antioxidants*, 2019, **8**(6), 174.
38 A. Procopio, C. Celia, M. Nardi, M. Oliverio, D. Paolino and G. Sindona, *J. Nat. Prod.*, 2011, **74**(11), 2377.
39 S. Bulotta, M. Celano, S. M. Lepore, T. Montalcini, A. Pujia and D. Russo, *J. Transl. Med.*, 2014, **12**, 219.
40 P. Plastina, C. Benincasa, E. Perri, A. Fazio, G. Augimeria, M. Poland, R. Witkamp and J. Meijerink, *Food Chem.*, 2019, **279**, 105.
41 T. Lian and R. J. Ho, *J. Pharm. Sci.*, 2001, **90**(6), 667.
42 B. Yang, Y. Dong, F. Wang and Y. Zhang, *Molecules*, 2020, **25**, 4613.
43 M. R. I. Shishir, N. Karim, V. Gowd, X. D. Zheng and W. Chen, *Trends Food Sci. Technol.*, 2019, **85**, 177.
44 R. Bernini, E. Mincione, M. Barontini and F. Crisante, *J. Agric. Food Chem.*, 2008, **56**(19), 8897.
45 V. Laghezza Masci, R. Bernini, N. Villanova, M. Clemente, V. Cicaloni, L. Tinti, L. Salvini, A. R. Taddei, A. Tiezzi and E. Ovidi, *Int. J. Mol. Sci.*, 2022, **23**(20), 12348.
46 M. Petaccia, D. Gradella Villalva, L. Galantini, C. Bombelli, L. Giansanti, G. Cerichelli and G. Mancini, *Colloids Surf., A*, 2015, **468**, 246.
47 O. Topel, B. Acar Çakır, L. Budama and N. Hoda, *J. Mol. Liq.*, 2013, **177**, 40.
48 S. Páll, A. Zhmurov, P. Bauer, M. Abraham, M. Lundborg, A. Gray, B. Hess and E. Lindahl, *J. Chem. Phys.*, 2020, **153**(13), 134110.
49 J. B. Klauda, R. M. Venable, J. A. Freites, J. W. O'Connor, D. J. Tobias, C. Mondragon-Ramirez, I. Vorobyov, A. D. J. MacKerell and R. W. Pastor, *J. Phys. Chem. B*, 2010, **114**(23), 7830.
50 W. L. Jorgensen, J. Chandrasekhar, J. D. Madura, R. W. Impey and M. L. Klein, *J. Chem. Phys.*, 1983, **79**(2), 926.
51 G. Bussi, D. Donadio and M. Parrinello, *J. Chem. Phys.*, 2007, **126**, 14101.
52 M. Parrinello and A. Rahman, *J. Appl. Phys.*, 1981, **52**(12), 7182.
53 R. C. MacDonald, and R. I. MacDonald, in *Liposome Technology*, ed. G. Gregoriadis, CRC Press, Boca Raton, Fl, USA, 2nd edn, 1992.
54 L. D. Mayer, M. J. Hope and P. R. Cullis, *Biochim. Biophys. Acta, Biomembr.*, 1986, **858**, 161.
55 J. D. Castile and K. M. G. Taylor, *Int. J. Pharm.*, 1999, **188**(1), 1999–87.
56 R. J. Hunter, in *Zeta Potential in Colloid Science. Principles and Applications*, ed. R. H. Ottewill, and R. L. Rowell, Elsevier, 1st edn, 1988.
57 G. Prevete, B. Simonis, M. Mazzonna, F. Mariani, E. Donati, S. Sennato, F. Ceccacci and C. Bombelli, *Biomolecules*, 2023, **13**(12), 1794.
58 M. Huang, J. Wang and C. Tan, *Int. J. Food Sci. Technol.*, 2022, **57**(5), 2701.
59 European Committee for Antimicrobial Susceptibility Testing (EUCAST) of the European Society of Clinical Microbiology and Infectious Diseases (ESCMID), Determination of minimum inhibitory concentrations (MICs) of antibacterial agents by broth dilution, *Clin. Microbiol. Infect.*, 2003, **9**(8), 9.
60 M. Bietti, E. Cucinotta, G. A. Di Labio, O. Lanzalunga, A. Lapi, M. Mazzonna, E. Romero-Montalvo and M. Salamone, *J. Org. Chem.*, 2019, **84**(4), 1778.
61 R. Re, N. Pellegrini, A. Proteggente, A. Pannala, M. Yang and C. Rice-Evans, *Free Radical Biol. Med.*, 1999, **26**(9), 1231.
62 N. Michel, A. S. Fabiano, A. Polidori, R. Jack and B. Pucci, *Chem. Phys. Lipids*, 2006, **139**(1), 11.
63 C. S. Velez-Saboyá, J. R. Guzmán-Sepúlveda and J. C. Ruiz-Suárez, *J. Phys.:Condens. Matter*, 2022, **34**(12), 124002.
64 S. Andrade, M. J. Ramalho, J. A. Loureiro and M. Carmo Pereira, *J. Mol. Liq.*, 2021, **324**, 114689.
65 O. Topel, B. Acar Çakır, L. Budama and N. Hoda, *J. Mol. Liq.*, 2013, **177**, 40.
66 K. S. Birdi, in *Handbook of Surface and Colloid Chemistry*, ed. K. S. Birdi, CRC Press, Boca Raton, 3rd edn, 2008.
67 Y. Nakahara, T. Kida, Y. Nakatsuji and M. Akashi, *Langmuir*, 2005, **21**(15), 6688.
68 J. B. Finean, *Chem. Phys. Lipids*, 1990, **54**, 147.
69 G. Bozzuto and A. Molinari, *Int. J. Nanomed.*, 2015, **10**(1), 975.
70 A. Magarkov, V. Dhawan, P. Kallinteri, T. Viitola, M. Elmowafy, T. Róg and A. Bunker, *Sci. Rep.*, 2014, **4**, 5005.

71 M. Petaccia, C. Bombelli, F. Paroni Sterbini, M. Papi, L. Giansanti, F. Bugli, M. Sanguinetti and G. Mancini, *Sens. Actuators, B*, 2017, **248**, 247.
72 L. Movileanu, I. Neagoe and M. L. Flonta, *Int. J. Pharm.*, 2000, **205**(1–2), 135.
73 Z. Bouallagui, M. Bouaziz and S. Lassoued, *Appl. Biochem. Biotechnol.*, 2011, **163**, 592.
74 L. Redondo-Morata, M. I. Giannotti and F. Sanz, *Langmuir*, 2012, **28**(35), 12851.
75 M. G. Benesch, D. A. Mannock, R. N. Lewis and R. N. McElhaney, *Biochem*, 2011, **50**(46), 9982.
76 W. Sułkowski, D. Pentak, K. Nowak and A. Sułkowska, *J. Mol. Struct.*, 2006, 257–264.
77 R. Amorati and L. Valgimigli, *Free Radical Res.*, 2015, **49**(5), 633.
78 R. Amorati, S. Menichetti, C. Viglianisi and M. C. Foti, *Chem. Commun.*, 2012, **48**, 11904.
79 Y. H. Fu, Y. Zhang, F. Wang, L. Zhao, G. B. Shen and X. Q. Zhu, *RSC Adv.*, 2023, **13**(5), 3295.
80 L. Valgimigli and R. Amorati, *Org. Biomol. Chem.*, 2012, **10**, 4147.
81 I. Nakanishi, T. Kawashima, K. Ohkubo, H. Kanazawa, K. Inami, M. Mochizuki, K. Fukuhara, H. Okuda, T. Ozawa, S. Itoh, S. Fukuzumi and N. Ikota, *Org. Biomol. Chem.*, 2005, **3**, 626.
82 L. Valgimigli, J. T. Banks, K. U. Ingold and J. Lusztyk, *J. Am. Chem. Soc.*, 1995, **117**, 9966.
83 A. S. Ulrich, M. Sami and A. Watts, *Biochim. Biophys. Acta*, 1994, **1191**(1), 225.
84 Z. E. Suntres, *J. Toxicol.*, 2011, 152474.
85 W. L. Stone and M. Smith, *Mol. Biotechnol.*, 2004, **27**(3), 217.
86 W. C. Lee and T. H. Tsai, *Int. J. Pharm.*, 2010, **395**(1), 78.
87 R. Natsuki, Y. Morita, S. Osawa and Y. Takeda, *Biol. Pharm. Bull.*, 1996, **19**(5), 758.
88 C. S. Tang, J. Y. Su, Z. P. Li, L. Z. Zhang, J. Yang, M. Qi, F. A. Liu and J. Tang, *Sci. China, Ser. B*, 1993, **36**(7), 809.
89 M. L. Corvo, O. C. Boerman, W. J. Oyen, L. Van Bloois, M. E. Cruz, D. J. Crommelin and G. Storm, *Biochim. Biophys. Acta*, 1999, **1419**(2), 325.
90 P. G. Sacks, V. Oke and K. Mehta, *J. Cancer Res. Clin. Oncol.*, 1992, **118**(7), 490.
91 Z. E. Suntres and P. N. Shek, *Crit. Care Med.*, 1998, **26**(4), 723.
92 Z. E. Suntres and P. N. Shek PN, *Biochem. Pharmacol.*, 2000, **59**(9), 1155.
93 J. Sinha, N. Das and M. K. Basu, *Biomed. Pharm.*, 2001, **55**(5), 264.